CRYSTAL GROWTH & DESIGN

Article

Relaxor-like Behavior and Structure Features of $Bi_2Ti_2O_7$ Pyrochlore Single Crystals

Alexander A. Bush, Mikhail V. Talanov,* Adam I. Stash, Sergey A. Ivanov, and Konstantin E. Kamentsev

Read Online

ACCESS | Metrics & More | Article Recommendations | Supporting Information

ABSTRACT: By slow cooling of the melt, large $Bi_2Ti_2O_7$ single crystals with a composition close to stoichiometric were grown. No traces of impurity phases were found on the X-ray diffraction patterns. A structural model with the space group $Fd\bar{3}m$ and displacive disorder in Bi-sublattice was proposed based on X-ray single crystal diffraction data. The dielectric properties of $Bi_2Ti_2O_7$ single crystals as a function of temperature at different frequencies were studied for the first time. As in the case of ceramic samples, a step-like frequency-dependent anomaly was detected at a temperature of about 220 K at a frequency of 1 kHz. It was found that attempts to describe the dielectric relaxation using the Arrhenius equation do not lead to physically significant values of the fitting parameters. However, the relaxation behavior is well described by the empirical Vogel–Fulcher relation, which is typical for many dipole and spin glasses, as well as relaxor ferroelectrics. Based on the value of fitting parameters, $Bi_2Ti_2O_7$ occupies an intermediate position between the canonical relaxor $PbMg_{1/3}Nb_{2/3}O_3$ on one hand and lead-free weakly coupled relaxors based on $BaTiO_3$ on the other one. Possible mechanisms of the observed relaxor-like behavior of the $Bi_2Ti_2O_7$ single crystal are discussed in terms of correlated hopping of bismuth cations and geometric frustration of the pyrochlore lattice.
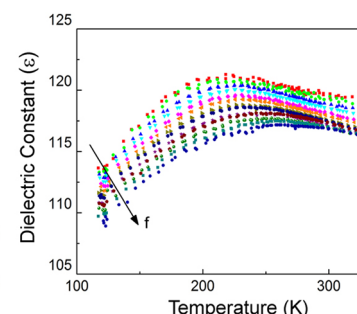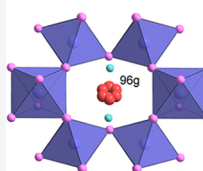
1. INTRODUCTION

Bismuth titanate $Bi_2Ti_2O_7$ is a pyrochlore-type compound, first synthesized in the 1960s,[1,2] and has attracted a remarkable amount of researcher attention due to its unusual dielectric and photocatalytic properties.[3−8] The combination of the relatively high dielectric constant ($\varepsilon \sim 100$), low dielectric loss, and low sintering temperature makes the title compound a promising material for using in multilayer ceramic capacitors, in storage capacitors of dynamic random access memory (DRAM), and as alternative gate insulating layers in advanced metal oxide semiconductor (MOS) transistors.[9,10] The temperature dependence ε of $Bi_2Ti_2O_7$ is characterized by a step-like frequency-dependent anomaly at $T \sim 200$ K, which was associated with a ferroelectric phase transition in some earlier studies.[11−13] However, later it was shown that $Bi_2Ti_2O_7$ is a linear dielectric, and the step-like frequency-dependent anomaly is not associated with a ferroelectric phase transition.[8]

A specific feature of the $Bi_2Ti_2O_7$ crystal structure is the disordered displacement of Bi^{3+} cations with a lone-electron pair from the Wyckoff position **16c** (Figure 1a,b) of the idealized cubic pyrochlore to the Wyckoff position **96g** (Figure 1c) or **96h** (with a 6-fold decrease in their occupancy), which is also characteristic of other Bi-containing pyrochlores.[14−16] Temperature-activated hopping of bismuth cations between six symmetrically equivalent positions can cause a step-like frequency-dependent anomaly according to some investigations.[17,18] A similar mechanism was previously proposed to
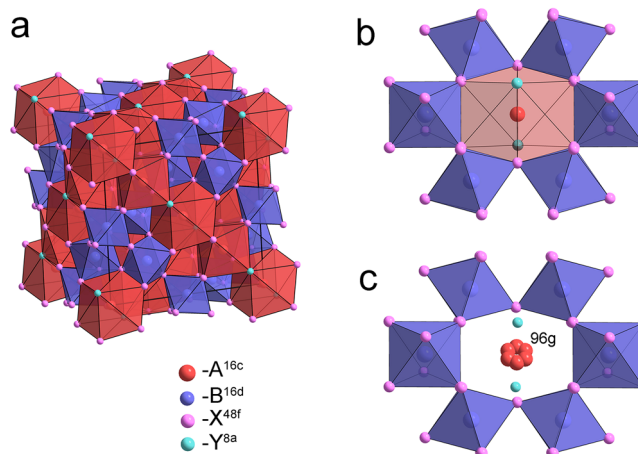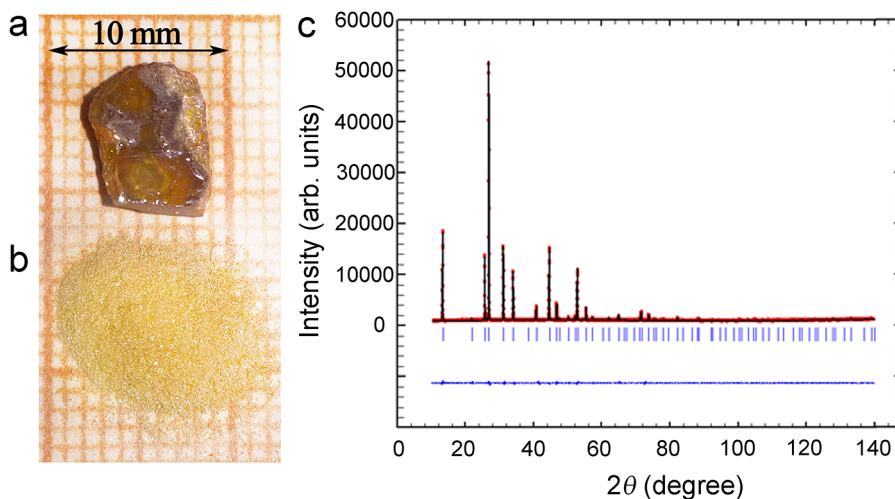

Figure 1. (a) Structure of an idealized cubic pyrochlore with the formula $A^{16c}_2B^{16d}_2X^{48f}_6Y^{8a}$ and with space group $Fd\bar{3}m$. (b) Local environment of the atom A^{16c} in the structure of idealized cubic pyrochlore. (c) Local environment of the atom Bi^{96g} in the structure of $Bi_2Ti_2O_7$ according to our experimental data.

- $-A^{16c}$
- $-B^{16d}$
- $-X^{48f}$
- $-Y^{8a}$

A

Figure 2. (a) Single crystal and (b) powder of $Bi_2Ti_2O_7$. (c) X-ray powder diffraction patterns for $Bi_2Ti_2O_7$. Observed X-ray data is given in red with the calculated pattern given in black. The difference between observed and calculated patterns is given in blue. The allowed peak positions are marked by the blue ticks.

explain dielectric relaxation in another Bi-containing pyrochlore $Bi_{1.5}Zn_{0.92}Nb_{1.5}O_{6.92}$ ($Bi_{1.5}Zn_{1.0}Nb_{1.5}O_7$)[19] and confirmed by comparing the results of dielectric measurements and IR spectroscopy.[20,21]

In the case of $Bi_2Ti_2O_7$ ceramics, the relaxation process (step-like frequency-dependent anomaly) was described using the Arrhenius equation with low attempt jump frequency ($\sim$1 MHz), which was associated with space charge polarization, but not with displacive disorder.[7] However, the manifestation of extrinsic effects, in particular, space charge polarization, is an integral part of the dielectric properties study of ceramic materials.[22−24] In addition, obtaining pure and high-density $Bi_2Ti_2O_7$ ceramic samples is a complex technological task due to the low temperature stability of the pyrochlore structure, which, according to Hector et al, is associated with a large ratio of ionic radii of Bi^{3+} and Ti^{4+} cations (1.93).[15] As a result, an increase in the annealing temperature by only 10 °C from the optimum value leads to the appearance of a significant amount ($\sim$19%) of the $Bi_4Ti_3O_{12}$ impurity phase.[15] The latter compound is a well-known high-temperature ferroelectric with a structure of the Aurivillius phase.[25−29] The presence of the $Bi_4Ti_3O_{12}$ impurity phase determines the visible "ferroelectric" properties of $Bi_2Ti_2O_7$ ceramics.[8,30]

The reasons that the off-centering tendency of the Bi^{3+} cations with a lone-electron pair in Bi-containing pyrochlores do not lead to long-range ordering of local distortions, as observed in many ferroelectric perovskites, are discussed from the point of view of the geometric frustration concept.[31,32] However, unlike many other Bi-containing pyrochlores exhibiting a temperature- and frequency-dependent dielectric relaxation (for example, $Bi_{1.5}Zn_{1.0}Nb_{1.5}O_7$[21] or $Bi_{1.56}Fe_{1.09}Nb_{1.15}O_7$[33]), there is no chemical disorder (disordered distribution of various ions at sites of equivalent crystallographic positions) in $Bi_2Ti_2O_7$. This allows us to separate the effect of chemical (compositional) disorder, which is characteristic of many relaxor ferroelectrics, from the possible manifestation of the geometric frustration characteristic of cationic sublattices in the structure of cubic pyrochlores. Thus, $Bi_2Ti_2O_7$ is a good model system for understanding polar phenomena in the bismuth pyrochlores.

A study of the structure and dielectric properties of pure $Bi_2Ti_2O_7$ single crystals would "shed light" on the origin of step-like frequency-dependent dielectric anomaly at $T \sim 200$ K, as well as contribute to understanding the fundamental role of geometric frustration in the formation of responses of nonmagnetic materials. However, up to now, there were no reports on the growth of large enough single crystals of $Bi_2Ti_2O_7$ for dielectric measurements with a composition close to the stoichiometric one. Earlier, Shimada et al.[34] reported the growth of $Bi_2Ti_2O_7$ crystals from melts containing Bi_2O_3, TiO_2, and V_2O_5 with the addition of 10 mol % ZnO. However, it was later shown that the composition of the crystals corresponds to the formula $Bi_{1.61}Zn_{0.18}Ti_{1.94}V_{0.06}O_{6.62}$ with the presence of impurities.[35] In this study, we report the growth of impurity-free large single crystals of $Bi_2Ti_2O_7$ and the results of the study of their structure features by X-ray single crystal diffraction. For the first time, the dielectric properties of $Bi_2Ti_2O_7$ single crystals were measured, and it was also shown that dielectric relaxation is described by the empirical Vogel−Fulcher law, which is typical for the canonical relaxors.

2. EXPERIMENTAL SECTION

Crystal Growth. Single crystals were grown using a slow cooling of the melt of a mixture of $(1 − x)Bi_2O_3 − xTiO_2$ with $x \sim 0.6$ in open yttrium-stabilized zirconium oxide crucibles in air atmosphere. At the same time, mixtures of Bi_2O_3 and TiO_2 oxides (analytical grade of purity, 99.0%) homogenized by grinding in an agate mortar in an ethyl alcohol medium were used as a batch. The size of the particles in the mixture was around 5–10 μm. The batch was placed in a cylindrical crucible with a capacity of 60 cm³; the degree of filling was 80% of its volume. Next, the batch was melted by heating it for 3 h to 1473 K; the melt was kept at this temperature for 1 h, then cooled to 1173 K at the rate of 7.5 K/h, and then cooled to room temperature with the furnace switched off.

The crystallized melt was a conglomerate of both crystals of $Bi_2Ti_2O_7$ and small plate-like crystals of $Bi_4Ti_3O_{12}$. It was possible to distinguish single crystals of the $Bi_2Ti_2O_7$ isometric habitus with sizes up to $3 \times 10 \times 10$ mm³ (Figure 2a). The single crystallinity of such samples was confirmed by the results of the registration of diffractograms in $\theta−2\theta$ geometry from them (see below), on which reflections from only one single crystal were found. The mirror-smooth most-developed face of the crystals coincides with the surface of the crystallized melt and is the (111) crystallographic plane in the

cubic setting. Traces of the impurity phase ($Bi_4Ti_3O_{12}$ impurity crystals) were present only in a thin layer on the surface of the solidified melt (Supporting Information, Figure S1). After cleaning the surface (for example, by etching it in acid), this peaks were absent. The milled powder obtained from the $Bi_2Ti_2O_7$ single crystal has a grayish yellow color (Figure 2b), which is also characteristic of the phase-pure samples.[8] Such a diffraction pattern without reflections of the impurity phase is shown in Figure 2c.

X-ray Single Crystal Diffraction. The experimental X-ray structural data set for the $Bi_2Ti_2O_7$ single crystal was obtained on a Bruker SMART APEX II automatic diffractometer equipped with an Oxford Cobra low-temperature cryosystem at a temperature close to room temperature (graphite monochromatic Mo K_α radiation, λ = 0.71073 Å, ω-scan, T = 290 K). Integration of X-ray diffraction peak intensities was carried out using the SAINT v 8.32B software; the SADABS v 2013 program included in the APEXII package[36] was used to take into account the absorption by crystal habitus, the reduction to a uniform scale, and the averaging of the integral intensities of the experimental data. Structural refinements were performed using SHELX-2014 software[37,38] using the XPREP utility to determine the correct space group. The model of crystal structure was refined by full-matrix least-squares over F^2hkl with anisotropic thermal parameters for all atoms. The parameters of the X-ray diffraction experiment and the final results of crystal structure refinements are presented in Table 1.

Table 1. Crystallographic and Experimental Data and Structure Refinement Parameters for a $Bi_2Ti_2O_7$ Crystal

Chemical formula	$Bi_2Ti_2O_7$
Molecular weight	625.76
Temperature (K)	290(2)
Crystal size (mm)	$0.245 \times 0.241 \times 0.084$
Crystal system	Cubic
Crystal shape	Triangular prism
Wavelength (Å)	0.71073
Space group	$Fd\bar{3}m$ (No 227)
a (Å)	10.3714(3)
V (Å^3)	1115.6(1)
Z	8
Number of measured reflections	7252
Number of independent reflections	246
Number of reflections with I > 2σ(I)	225 (R_{int} = 0.059)
θ (deg)	3.402–44.335
Absorption coefficient (μ) (mm^{-1})	65.648
Number of specified parameters	16
R (I > 2σ(I))	0.0522
wR (I > 2σ(I))	0.1139
GOOF	1.396

X-ray Powder Diffraction. The phase identification and purity of the powder prepared from single crystal was checked from the X-ray powder diffraction (XRPD) patterns obtained on a Bruker D8 Advance diffractometer (Vantec position-sensitive detector, Ge-monochromatized Cu K_β radiation, Bragg–Brentano geometry, DIFFRACT plus software) in the 2θ range 5–140° with a step size of 0.02° (counting time was 15 s per step). XRPD patterns (Figure 2) were analyzed with the full-profile Rietveld profile method

implemented in the FULLPROF software.[39] The diffraction peaks were described by a pseudo-Voigt profile function, with a Lorentzian contribution to the Gaussian peak shape. A peak asymmetry correction was made for angles below 35° (2θ). Background intensities were estimated by interpolating between up to 40–50 selected points or described by a polynomial with six coefficients.

The microstructure of the crystals was characterized by a scanning electron microscope (SEM) (JEOL, JSM6510LV).

Analysis of Chemical Composition. ICP-AES Jobin-Yvon JY 70 spectrometer was used to determine a real cation composition of single crystals. Crystals were fused with $LiBO_2$ and dissolved in HNO_3. Ten measurements per sample were made and the average plus standard deviation (SD) values were taken. Typical analytical precision was better than 1% of the measured values. The total amount of impurity cations did not exceed 0.05 at %. According to the elemental analyses done on different crystallites, the metal compositions of $Bi_2Ti_2O_7$ samples follow, if the sum of the cations is assumed to be 4 (at % Bi, 49.91(3); Ti, 50.09(3)). These values are very close to the expected ratios and permit us to conclude that sample stoichiometry is identical to the nominal case.

Dielectric Measurement. Dielectric measurements were carried out using an E7-20 immittance meter (Minsk Scientific Research Instrument Making Institute, Belarus) at electric field frequencies of $25–10^6$ Hz in the temperature range 4.2−1000 K. The sample was in the form of a rectangular plate with the sizes of $4 \times 4 \times 1$ mm^3. The base surface of the sample was covered by the electrodes which were obtained by burning Ag-paste at ∼773 K. A special measuring cell was used in which the sample was attached to the Pt plates by means of a soft spring. Data on the resistance (Figure S2) were calculated from the data on dielectric permittivity ε and the tangent of dielectric loss angle tan δ by the formula $\rho = 1/2\pi f \varepsilon \varepsilon_0 \tan \delta$, where f is the frequency of the measuring field, and ε_0 is electric constant.

The X-ray powder diffraction pattern registered from the sample after these measurements showed that there was no phase decomposition at the stage of this measuring process.
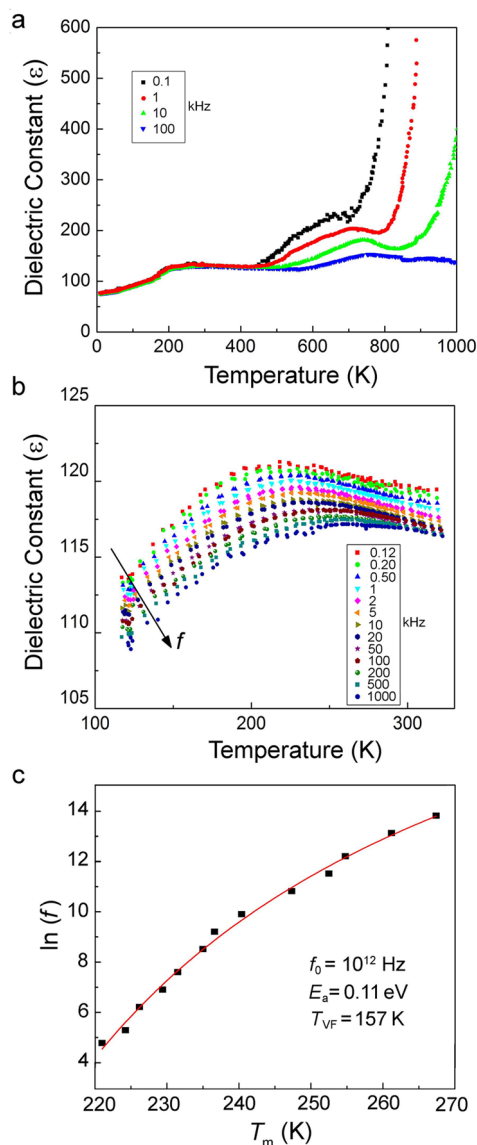
3. RESULTS AND DISCUSSION

XRD on $Bi_2Ti_2O_7$ single crystals at room temperature revealed that they retain the cubic pyrochlore structure with space group $Fd\bar{3}m$ (Table 1). The results of the X-ray diffraction analysis of $Bi_2Ti_2O_7$ crystals (Table 2) have much in common with the models proposed on the basis of Rietveld refinements of X-ray and neutron powder diffraction data.[15,40] First of all, we found that Bi cations are displaced from the Wyckoff position **16c** with local symmetry $\bar{3}m$ in the {111} plane by 0.3895 Å and occupy the Wyckoff position (**96g**) with local symmetry m. Note that a similar Wyckoff position for bismuth cations was proposed based on the X-ray powder diffraction study[15] and first-principles calculations.[8] However, in a number of studies, Wyckoff position **96h**[40−42] is used for bismuth cations, which is pointed between nearby **48f** anions (Wyckoff position **96g** shifted to the nearest **48f** anion; see Figure 1c).

Since the model of the structure of this compound was proposed earlier, we decided to thoroughly investigate the structural model proposed by Hector and Wiggin (see the table with its structural parameters[15]) and compare with our model. So, let us start our setup with their experimental details.

Table 2. Atomic Coordinates Occupation Factors and Isotropic Thermal Parameters for $Bi_2Ti_2O_7$

atom	Wyckoff position	x	y	z	occupancy	U_{iso}, (Å)
Bi	96g	0.0158(4)	0.0158(4)	0.9697(4)	0.1667	0.0191(6)
Ti	16d	0	1/4	3/4	1.000	0.0100(4)
O1	48f	0.1810(6)	−1/8	7/8	1.000	0.0147(9)
O2	8a	−1/8	−1/8	7/8	0.72(10)	0.052(14)

We used modern single crystal X-ray diffractometer with a fairly accurate measurement of the structural amplitudes; our crystal was definitely single-domain. Owing to the cubic symmetry of $Bi_2Ti_2O_7$ crystal, a large number of equivalent reflections was measured, the averaging of which allowed us to reliably refine the structure by the method of least-squares (more than 10 reflections per refined parameter). The possible disadvantages of our experiment include the fact that X-rays are in principle not particularly sensitive for the determination of the parameters of the oxygen sublattice in the structures with heavy cations. We also note that the crystal was not isometric, which allowed us to estimate the absorption correction with a certain error.

In the case of investigation performed in ref 15, the authors used the neutron powder diffraction method. Neutrons are quite sensitive to oxygen, and this allowed them to hope for an accurate determination of the coordinates and populations of oxygen. However, their sample was not single crystal, and moreover, there was an impurity $Bi_4Ti_3O_{12}$ in the powder, which probably led to a violation of the stoichiometry of the studied sample. The Rietveld method which was mainly used in this research is based on the knowledge of a certain initial model, which is a significant limitation of the method. In our case, we obtained a model directly from a set of intensities without binding it to previously defined structural models.

As a result of our crystal structure determination, a statistically significant structure model was found. The Bi cation is shifted from a highly symmetric position due to a lone-electron pair. Regarding oxygen, we tried to add some kind of disorder, but all attempts did not allow us to make a certain conclusion because of its weak influence on the diffraction pattern. So, the question with O_2 oxygen ordering is still unanswered. The increased value of the thermal parameter can be an indicator of disorder, but the position of the split oxygen can be determined only by difference synthesis maps, when all previously defined atoms are subtracted. In our experiment, nothing like O_2 splitting could be determined, but it is important to note that for our crystal, the refined occupation factor of O_2 is not complete (0.72 (10) instead of 1.0). There is probably a slight oxygen deficiency, but additional measurements (neutrons, DTA, iodometric titration) are needed to confirm this conclusion.

In the model proposed in ref 15, O_2 was artificially split. The effect of this disorder is not evident because the thermal parameters for these splitting anions are still rather large in comparison with Bi and Ti. At the same time, all other atoms of the model[15] are defined (within their accuracy) correctly and are consistent with ours.

Figure 3a shows the temperature dependence of the dielectric constant (ε) for the $Bi_2Ti_2O_7$ single crystal measured at different frequencies on cooling. There are two dielectric anomalies: a strongly relaxing maximum at $T = 500-800$ K and a step-like frequency-dependent anomaly at $T \approx 200$ K. The high-temperature anomaly is characterized by a significant shift in the maximum temperature (T_m) (more than 150 K) with frequency. A similar low-frequency behavior of the dielectric constant was observed in many oxide dielectrics and is associated with an increase in conductivity with increasing temperature and relaxation of the space charge.[22] In our case, there is also a sharp increase in conductivity at $T > 500$ K by more than 3 orders of magnitude (Supporting Information, Figure S2).

Figure 3. (a) Temperature dependences of the dielectric constant measured upon cooling at different frequencies in the $Bi_2Ti_2O_7$ single crystal. (b) Step-like frequency-dependent anomaly of the $Bi_2Ti_2O_7$ single crystal. (c) Plots of $\ln(f)$ vs T_m and VF relation fitting (red line).

Step-like frequency-dependent anomaly is observed at $T = 220$ K at $f = 1$ kHz (Figure 3b), which is comparable with previous results obtained on the ceramic samples.[7,8] The maximum values of ε are 116 (at $f = 500$ kHz), and $\tan \delta < 0.01$, which is also very close to the results in the indicated works, where $\varepsilon = 115$.[8] However, we also note the differences: at frequencies less than 10 kHz, no additional anomaly is observed at $T > 200$ K, as in ref 7. As f increases, the dielectric maximum temperature (T_m) shifts by more than 50 K, and the shape of the step-like frequency-dependent anomaly is smoothed. Attempts to describe the behavior of the T_m frequency dependence using the Arrhenius equation led to physically insignificant values of the attempts frequency to overcome the potential barrier $f_0 \sim 10^{25}$ (Table 3, Supporting Information, Figure S3). An attempt to isolate two relaxation processes described by Arrhenius equations with different parameters (Table 3, Supporting Information, Figure S4) led

Table 3. Fitting Parameters of the Arrhenius and Vogel–Fulcher laws for the $Bi_2Ti_2O_7$ Single Crystal

	f_0 (Hz)	E_a (eV)	T_{VF} (K)	R_{adj}^2
Arrhenius	4.5×10^{25}	1.05	-	0.972
Arrhenius (2)	5.1×10^{21}	0.83	-	0.988
	6.8×10^{30}	1.27		0.991
Vogel-Fulcher	1×10^{12}	0.11	157	0.994

to a similar result. However, obtained experimental results are well described (with $R_{adj}^2 = 0.994$, R_{adj} is the adjusted coefficient of determination) by the empirical Vogel–Fulcher relation (Table 3, Figure 3c)

$$f = f_0 \exp[-E_a/k(T_m - T_{VF})]$$

where f_0 is the attempted frequency to overcome the potential barrier; E_a is the activation energy; k is Boltzmann constant, T_{VF} is the Vogel–Fulcher temperature. In the canonical relaxor $PbMg_{1/3}Nb_{2/3}O_3$, these parameters have a clear physical meaning; in particular, T_{VF} is associated with the freezing temperature of dipole reorientation dynamics and transition in the non-ergodic relaxor state on cooling.[43] However, as shown by Tagantsev,[44] the Vogel–Fulcher law for the frequency dependences of T_m (in contrast to the temperature dependences of the relaxation time) can also be observed in systems without freezing the dynamics of the dipoles. Therefore, to establish the real mechanisms of dielectric relaxation in the $Bi_2Ti_2O_7$, investigation of the temperature dependence of the relaxation time in a wide frequency range, as well as distribution function, is necessary. Nevertheless, using the Vogel–Fulcher law to describe the frequency dependences of T_m and comparing the corresponding fitting parameters are convenient tools for comparing relaxor-like materials.

In the case of the $Bi_2Ti_2O_7$ single crystals, $f_0 \sim 10^{12}$ is on the order of phonon frequency and is comparable with the results obtained for other Bi-containing pyrochlores (BZN) from the Arrhenius analysis.[20,21,45] The value of $E_a = 0.11$ eV is higher than the value determined for the canonical relaxor $PbMg_{1/3}Nb_{2/3}O_3$ ($E_a = 0.76$ eV),[46] but is very close to the parameters of many lead-free relaxors,[47] in particular to $(1 - x)$ $BaTiO_3 - x BaSnO_3$[48] and $(1 - x)$ $BaTiO_3 - x BaZrO_3$[49] at $x = 0.3$ and $x = 0.4–0.5$, respectively. We also note the qualitative similarity of the temperature dependences of the dielectric constant for $Bi_2Ti_2O_7$ single crystals and $(1 - x)$ $BaTiO_3 - x BiScO_3$ solid solutions with $x = 0.2–0.4$.[50] However, due to the large values of E_a (~ 0.25 eV), as well as high coercive fields and low remanent polarization, the latter were assigned to a weakly coupled relaxor. Thus, $Bi_2Ti_2O_7$ in terms of the fitting parameter E_a occupies an intermediate position between the canonical relaxor $PbMg_{1/3}Nb_{2/3}O_3$ on one hand and lead-free weakly coupled relaxors based on $BaTiO_3$ on the other.

The value of $T_{VF} = 157$ K is lower than the maximum temperature of the step-like frequency-dependent anomaly by more than 50 K. In the canonical relaxor $PbMg_{1/3}Nb_{2/3}O_3$, the value of T_{VF} corresponds to the transition temperature from the ergodic to non-ergodic relaxor state upon cooling,[43] wherein the macroscopic structure of $PbMg_{1/3}Nb_{2/3}O_3$ remains cubic up to 5 K with decreasing temperature.[51,52] In the case of many other relaxors, for example, $PbZn_{1/3}Nb_{2/3}O_3$ and $(1 - x)$ $PbMg_{1/3}Nb_{2/3}O_3 - x PbTiO_3$ with $x \sim 0.25$, a diffuse transition to the ferroelectric phase takes place upon cooling, rather than the transition to the non-ergodic relaxor

state. In this case, the determined value of the T_{VF} parameter does not have a clear physical meaning, and the dielectric relaxation mechanisms are not associated with the freezing of the dipole dynamics.[53] However, this is accompanied by symmetry lowering of the macroscopic crystal structure, while $Bi_2Ti_2O_7$ (like $PbMg_{1/3}Nb_{2/3}O_3$) is cubic down to low temperatures without undergoing the ferroelectric phase transition.[15]

Note that, despite the very close values of the parameters E_a and f_0 in $Bi_2Ti_2O_7$ and in $Bi_{1.5}Zn_{1.0}Nb_{1.5}O_7$ ($E_a \sim 0.2$ eV, $f_0 \sim 10^{12}$ Hz[21]), the nature of the manifestation of the dielectric relaxation in them is fundamentally different. For $Bi_{1.5}Zn_{1.0}Nb_{1.5}O_7$, the temperature behavior at the low-frequency end of the distribution of Debye relaxation frequencies obeys the Arrhenius law, which implies that the charges hop independently of each other.[54] Attempts to use the Vogel–Fulcher law for $Bi_{1.5}Zn_{1.0}Nb_{1.5}O_7$ were unsuccessful in the case of films[55] or led to insignificant $T_{VF} = 0.4$ K in the case of ceramics,[21] confirming the correctness of the Arrhenius law fitting. In $Bi_2Ti_2O_7$, on the contrary, the T_{VF} value is significant, and the use of the Arrhenius law cannot lead to physically meaningful fitting parameters (Table 3). This means that the correlation effects between dipoles (or hopping motion) cannot be neglected.

According to the first-principle calculations, bismuth ions hopping between symmetrically equivalent positions separated by an energy barrier of 0.11–0.21 eV are the source of dielectric relaxation in $Bi_2Ti_2O_7$.[17] Then, taking into account our dielectric spectroscopy data, we can assume the existence of a correlation between the temperature-induced hopping of various bismuth ions. The existence of a correlation between the static displacements of neighboring bismuth atoms was also reported.[41] This work claims that $\angle Bi–Bi$ for neighboring displacements has a preference for 180° alignment, which corresponds to zigzag ordering. A similar correlation between Bi-displacements was found in the first-principles study of $Bi_2Ti_2O_7$.[56] The β-crystoballite-type orientational disorder in the Bi_2O' substructure was also found in other Bi-containing pyrochlores,[57−59] and it is believed that strongly correlated displacements within Bi_4O' tetrahedrons affect the manifestation of dielectric properties.[19,57] A recent work notes the universal nature of such displacements within the pyrochlore structure with an emphasis on the manifestation of structural frustration and the lack of ferroelectric behavior in pyrochlores.[60]

It is well-known that cations with a lone pair of electrons, such as Bi^{3+} and Pb^{2+}, tend to have off-center shifts. Coherent lone pair displacements produce a ferroelectric ground state in the case of textbook compounds $PbTiO_3$ and $Bi_4Ti_3O_{12}$ with the structure of perovskite and the Aurivillius phase, respectively. The structure of the idealized cubic pyrochlore $A^{16c}_2B^{16d}_2X^{48f}_6Y^{8a}$ with the space group $Fd\bar{3}m$ is characterized by the interconnected tetrahedra network formed by atoms at Wyckoff positions 16d and 16c (in $Bi_2Ti_2O_7$, the bismuth ion is shifted to position 96g (Table 2, Figure 4a)).[61] Such a crystalline structure is frustrated, and if antiferromagnetically coupled magnetic ions are located at the vertices of the tetrahedra, then spin-liquid or spin-glass behavior will be expected.[62,63] If the network of tetrahedra is formed by ions with a lone pair of electrons, then their coherent off-centering distortions are frustrated and the transition to the ferroelectric state is suppressed.[31] By analogy with magnetic systems, the term "charge-ice" was proposed for pyrochlore containing ions
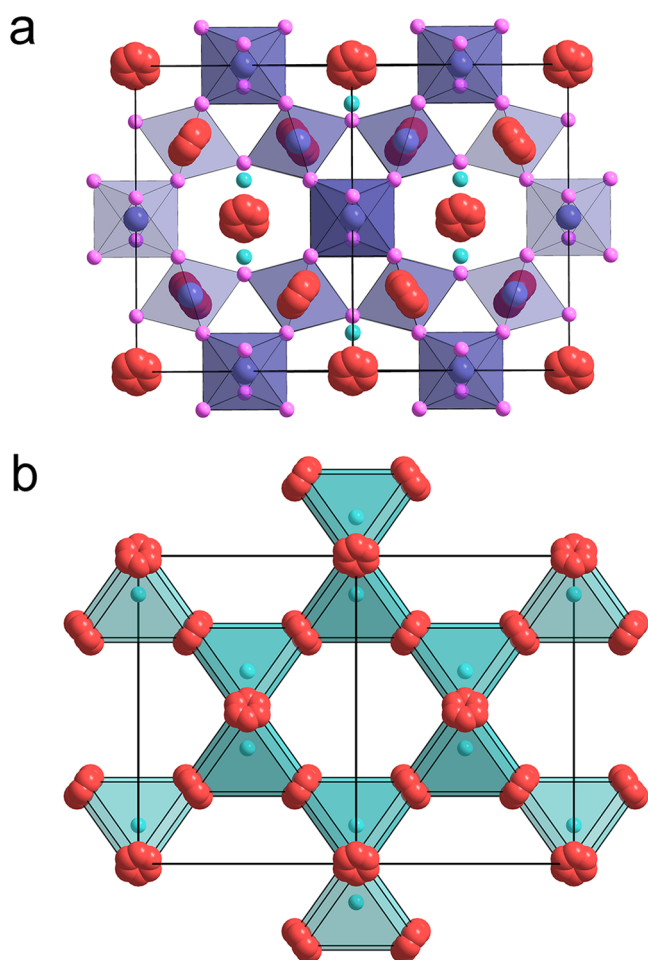
Figure 4. (a) Crystal structure of the $Bi_2Ti_2O_7$ single crystal along the [110] direction at room temperature. Bi atoms and Ti atoms are shown by red and deep blue color, respectively; O1 atoms and O2 atoms are shown by purple and cyan color, respectively. (b) Interconnected tetrahedra network formed by Bi atoms. Only the shortest Bi−Bi distances in tetrahedra are shown.

with a lone pair of electrons.[31] Apparently, a similar situation occurs in $Bi_2Ti_2O_7$ (Figure 4b), in which incoherent Bi off-centering was detected and investigated by reverse Monte Carlo structural analysis using total neutron scattering.[42] The presence of additional disorder in $Bi_2Ti_2O_7$ arising from incoherent frozen displacements of the Bi^{3+} ions is connected with the observed suppression of excess specific heat at low temperature by Melot et al.[32]

By taking into account the concept developed in refs 31,32, $Bi_2Ti_2O_7$ can be considered in parallel with relaxor ferroelectrics, in particular, with the canonical relaxor $PbMg_{1/3}Nb_{2/3}O_3$, in which a long-range ferroelectric order is suppressed by substitutional disorder. The disordered distribution of Mg^{2+} and Nb^{5+} ions at crystallographically equivalent positions can lead to the appearance in the system of frustrated interactions (ferroelectric and antiferroelectric) between polar nanoregions with a short-range ferroelectric order. $Bi_2Ti_2O_7$, on the contrary, is a well-ordered system, and the frustration in it is a consequence of the specific geometry of the crystal lattice (geometric frustration), which is characteristic of the structure of cubic pyrochlore. In both $Bi_2Ti_2O_7$ and $PbMg_{1/3}Nb_{2/3}O_3$, a decrease in temperature does not lead to a transition to a long-range-ordered ferroelectric state, and

dielectric relaxation is described by the empirical Vogel−Fulcher relation. Cooling $PbMg_{1/3}Nb_{2/3}O_3$ below T_{VF} leads to the transition to the non-ergodic relaxor state.[43] However, the method used to estimate the dielectric relaxation in $Bi_2Ti_2O_7$ does not allow us to interpret the physical meaning of the fitting parameters of the Vogel−Fulcher law, in particular, T_{VF}. For this reason, the nature of the low-temperature state of $Bi_2Ti_2O_7$ is unclear and requires further study using methods of broadband dielectric spectroscopy.

4. CONCLUSIONS

Large impurity-free $Bi_2Ti_2O_7$ single crystals were grown by slow cooling of a melt of a Bi_2O_3−TiO_2 mixture. Using X-ray single crystal diffraction, the $Bi_2Ti_2O_7$ structure was established at room temperature and its cubic symmetry with the space group $Fd\bar{3}m$ was confirmed. Bismuth cation is shifted from a highly-symmetry **16c** Wyckoff position to a **96g** one, which confirms the displacive disorder in the structure of the single crystals. The dielectric properties of $Bi_2Ti_2O_7$ single crystals were studied for the first time, and it was shown that, as in the case of ceramics, a step-like frequency-dependent anomaly at T = 220 K (at f = 1 kHz) is observed. It was found that attempts to describe the frequency dependence of T_m for $Bi_2Ti_2O_7$ single crystals using the Arrhenius equation lead to physically insignificant fitting parameters. However, it was found that frequency dispersion of T_m is well-described by the empirical Vogel−Fulcher relation, which is typical for many relaxors. By the value of E_a, $Bi_2Ti_2O_7$ is intermediate between the canonical relaxor $PbMg_{1/3}Nb_{2/3}O_3$ on one hand and lead-free weakly coupled relaxors based on $BaTiO_3$ on the other. With the conclusion that the cause of dielectric relaxation in Bi-containing pyrochlores is the temperature-activated hopping of bismuth atoms between six symmetrically equivalent positions[17−21] taken into account, our data suggest the existence of a correlation between hopping of various bismuth ions in $Bi_2Ti_2O_7$. The discovered relaxor-like behavior of the $Bi_2Ti_2O_7$ single cryslal makes it a candidate-material for studying aspects of geometric frustration in nonmagnetic systems and their effect on the suppression of long-range ferroelectric order.

■ ASSOCIATED CONTENT

ⓢ Supporting Information

The Supporting Information is available free of charge at https://pubs.acs.org/doi/10.1021/acs.cgd.9b01220.

> X-ray diffraction patterns of the powdered crystals and single crystal of $Bi_2Ti_2O_7$ (S1). Temperature dependence of the electrical resistance of $Bi_2Ti_2O_7$ single crystal (S2). The plots of $\ln(f)$ vs T_m and fitting with Arrhenius equation for one (S3) and for two (S4) relaxation processes. (PDF)

■ AUTHOR INFORMATION

Corresponding Author

Mikhail V. Talanov − *Southern Federal University, Rostov-on-Don, Russia;* ◉ orcid.org/0000-0002-5416-9579; Email: mvtalanov@gmail.ru

Other Authors

Alexander A. Bush − *MIREA − Russian Technological University (RTU MIREA), Moscow, Russia*

Adam I. Stash − *A. N. Nesmeyanov Institute of Organoelement Compounds of Russian Academy of Science, Moscow, Russia*

Sergey A. Ivanov − *N.N. Semenov Institute of Chemical Physics, Moscow, Russia*

Konstantin E. Kamentsev − *MIREA − Russian Technological University (RTU MIREA), Moscow, Russia*

Complete contact information is available at:
https://pubs.acs.org/10.1021/acs.cgd.9b01220

Notes

The authors declare no competing financial interest.

■ REFERENCES

(1) Aleshin, E.; Roy, R. Crystal Chemistry of Pyrochlore. *J. Amer. Ceram. J. Am. Ceram. Soc.* **1962**, *45*, 18−25.

(2) Knop, O.; Brisse, F.; Castelliz, L. Pyrochlores V. Thermoanalytic, X-ray, neutron, infrared, and dielectric studies of $A_2Ti_2O_7$ titanates. *Can. J. Chem.* **1969**, *47*, 971−990.

(3) Gupta, S.; Subramanian, V. Encapsulating $Bi_2Ti_2O_7$ (BTO) with reduced graphene oxide (RGO): an effective strategy to enhance photocatalytic and photoelectrocatalytic activity of BTO. *ACS Appl. Mater. Interfaces* **2014**, *6*, 18597−18608.

(4) Yao, W. F.; Wang, H.; Xu, X. H.; Zhou, J. T.; Yang, X. N.; Shu, Y. Z.; Shang, X. Photocatalytic property of bismuth titanate $Bi_2Ti_2O_7$. *Appl. Catal., A* **2004**, *259*, 29−33.

(5) Bian, Z.; Huo, Y.; Zhang, Y.; Zhu, J.; Lu, Y.; Li, H. Aerosol-spray assisted assembly of $Bi_2Ti_2O_7$ crystals in uniform porous microspheres with enhanced photocatalytic activity. *Appl. Catal., B* **2009**, *91*, 247−253.

(6) Bencina, M.; Valant, M. $Bi_2Ti_2O_7$-based pyrochlore nanoparticles and their superior photocatalytic activity under visible light. *J. Am. Ceram. Soc.* **2018**, *101*, 82−90.

(7) Turner, C. G.; Esquivel-Elizondo, J. R.; Nino, J. C. Dielectric Properties and Relaxation of $Bi_2Ti_2O_7$. *J. Am. Ceram. Soc.* **2014**, *97*, 1763−1768.

(8) Esquivel-Elizondo, J. R.; Hinojosa, B. B.; Nino, J. C. $Bi_2Ti_2O_7$: It Is Not What You Have Read. *Chem. Mater.* **2011**, *23*, 4965−4974.

(9) Jing, X.; Huang, B.; Yang, X.; Wei, J.; Wang, Z.; Wang, P.; Zheng, L.; Xu, Z.; Liu, H.; Wang, X. Growth and electrical properties of Ce-doped $Bi_2Ti_2O_7$ thin films by chemical solution deposition. *Appl. Surf. Sci.* **2008**, *255*, 2651−2654.

(10) Hwang, G. W.; Kim, W. D.; Min, Y.-S.; Cho, Y. J.; Hwang, C. S. Characteristics of Amorphous $Bi_2Ti_2O_7$ Thin Films Grown by Atomic Layer Deposition for Memory Capacitor Applications. *J. Electrochem. Soc.* **2006**, *153*, F20−F26.

(11) Hou, Y.; Wang, M.; Xu, X.-H.; Wang, D.; Wang, H. Dielectric and Ferroelectric Properties of Nanocrystalline $Bi_2Ti_2O_7$ Prepared by a Metalloorganic Decomposition Method. *J. Am. Ceram. Soc.* **2002**, *85*, 3087−3089.

(12) Yordanov, S. P.; Ivanov, I.; Carapanov, Ch. P. Dielectric properties of the ferroelectric $Bi_2Ti_2O_7$ ceramics. *J. Phys. D: Appl. Phys.* **1998**, *31*, 800−806.

(13) Kim, S. S.; Park, M. H.; Chung, J. K.; Kim, W.-J. Structural study of a sol-gel derived pyrochlore $Bi_2Ti_2O_7$ using a Rietveld analysis method based on neutron scattering studies. *J. Appl. Phys.* **2009**, *105*, 061641.

(14) Avdeev, M.; Haas, M. K.; Jorgensen, J. D.; Cava, R. J. Static disorder from lone-pair electrons in $Bi_{2-x}M_xRu_2O_{7-y}$ (M = Cu; Co; x = 0; 0.4) pyrochlores. *J. Solid State Chem.* **2002**, *169*, 24−34.

(15) Hector, A. L.; Wiggin, S. B. Synthesis and structural study of stoichiometric $Bi_2Ti_2O_7$ pyrochlore. *J. Solid State Chem.* **2004**, *177*, 139−145.

(16) Krayzman, V.; Levin, I.; Woicik, J. C. Local Structure of Displacively Disordered Pyrochlore Dielectrics. *Chem. Mater.* **2007**, *19*, 932−936.

(17) Brooks Hinojosa, B.; Asthagiri, A.; Nino, J. C. Capturing dynamic cation hopping in cubic pyrochlores. *Appl. Phys. Lett.* **2011**, *99*, 082903.

(18) Brooks Hinojosa, B.; Asthagiri, A.; Nino, J. C. Energy landscape in frustrated systems: Cation hopping in pyrochlores. *Appl. Phys. Lett.* **2013**, *103*, 022901.

(19) Levin, I.; Amos, T. G.; Nino, J. C.; Vanderah, T. A.; Randall, C. A.; Lanagan, M. T. Structural Study of an Unusual Cubic Pyrochlore $Bi_{1.5}Zn_{0.92}Nb_{1.5}O_{6.92}$. *J. Solid State Chem.* **2002**, *168*, 69−75.

(20) Nino, J. C.; Lanagan, M. T.; Randall, C. A.; Kamba, S. Correlation between infrared phonon modes and dielectric relaxation in Bi_2O_3-ZnO-Nb_2O_5 cubic pyrochlore. *Appl. Phys. Lett.* **2002**, *81*, 4404−4406.

(21) Kamba, S.; Porokhonskyy, V.; Pashkin, A.; Bovtun, V.; Petzelt, J.; Nino, J. C.; Trolier-McKinstry, S.; Lanagan, M. T.; Randall, C. A. Anomalous broad dielectric relaxation in $Bi_{1.5}Zn_{1.0}Nb_{1.5}O_7$ pyrochlore. *Phys. Rev. B: Condens. Matter Mater. Phys.* **2002**, *66*, 054106.

(22) Elissalde, C.; Ravez, J. Ferroelectric ceramics: defects and dielectric relaxations. *J. Mater. Chem.* **2001**, *11*, 1957−1967.

(23) Ang, C.; Yu, Z.; Cross, L. E. Oxygen-vacancy-related low-frequency dielectric relaxation and electrical conduction in Bi: $SrTiO_3$. *Phys. Rev. B: Condens. Matter Mater. Phys.* **2000**, *62*, 228−236.

(24) Jonscher, A. K. Dielectric relaxation in solids. *J. Phys. D: Appl. Phys.* **1999**, *32*, R57−R70.

(25) Smolensky, G. A.; Isupov, V. A.; Agranovskaya, A. I. Ferroelectrics of the Oxygen-Octahedral Type with Layered Structure. *Sov. Phys. Solid State (Engl. Trans.)* **1961**, *3*, 651−655.

(26) Subba Rao, E. C. Ferroelectricity in $Bi_4Ti_3O_{12}$ and Its Solid Solution. *Phys. Rev.* **1961**, *122*, 804−807.

(27) Subba Rao, E. C. A Family of Ferroelectric bithmuth compounds. *J. Phys. Chem. Solids* **1962**, *23*, 665−676.

(28) Paz de Araujo, C. A.; Cuchiaro, J. D.; McMillan, L. D.; Scott, M. C.; Scott, J. F. Fatigue-Free Ferroelectric Capacitors with Platinum Electrodes. *Nature* **1995**, *374*, 627−629.

(29) Shirokov, V. B.; Talanov, M. V. Phase transitions in $Bi_4Ti_3O_{12}$. *Acta Crystallogr., Sect. B: Struct. Sci., Cryst. Eng. Mater.* **2019**, *75*, 978−986.

(30) Su, W.-F.; Lu, Y.-T. Synthesis, phase transformation and dielectric properties of sol-gel derived $Bi_2Ti_2O_7$ ceramics. *Mater. Chem. Phys.* **2003**, *80*, 632−637.

(31) Seshadri, R. Lone pairs in insulating pyrochlores: Ice rules and high-k behavior. *Solid State Sci.* **2006**, *8*, 259−266.

(32) Melot, B. C.; Tackett, R.; O'Brien, J.; Hector, A. L.; Lawes, G.; Seshadri, R.; Ramirez, A. P. Large low-temperature specific heat in pyrochlore $Bi_2Ti_2O_7$. *Phys. Rev. B: Condens. Matter Mater. Phys.* **2009**, *79*, 224111.

(33) Lufaso, M. W.; Vanderah, T. A.; Pazos, I. M.; Levin, I.; Roth, R. S.; Nino, J. C.; Provenzano, V.; Schenck, P. K. Phase formation, crystal chemistry, and properties in the system Bi_2O_3-Fe_2O_3-Nb_2O_5. *J. Solid State Chem.* **2006**, *179*, 3900−3910.

(34) Shimada, S.; Kodaira, K.; Matsushita, T. Crystal growth of bismuth titanates and titanium oxide from melts in the system Bi_2O_3-V_2O_5-TiO_2. *J. Cryst. Growth* **1977**, *41*, 317−320.

(35) Kahlenberg, V.; Böhm, H. X-ray diffraction investigation of the defect pyrochlore $Bi_{1.61}Zn_{0.18}Ti_{1.94}V_{0.06}O_{6.62}$. *J. Alloys Compd.* **1995**, *223*, 142−146.

(36) APEX II; Bruker AXS Inc.: Madison, WI, 2014.

(37) Sheldrick, G. M. A short history of SHELX. *Acta Crystallogr., Sect. A: Found. Crystallogr.* **2008**, *64*, 112−122.

(38) Sheldrick, G. M. Crystal structure refinement with SHELXL. *Acta Crystallogr., Sect. C: Struct. Chem.* **2015**, *71*, 3−8.

(39) Rodriguez-Carvajal, J. Recent advances in magnetic structure determination by neutron powder diffraction. *Phys. B* **1993**, *192*, 55−69.

(40) Radosavljevic, I.; Evans, J. S. O.; Sleight, A. W. Synthesis and Structure of Pyrochlore-Type Bismuth Titanate. *J. Solid State Chem.* **1998**, *136*, 63−66.

(41) Shoemaker, D. P.; Seshadri, R.; Hector, A. L.; Llobet, A.; Proffen, T.; Fennie, C. J. Atomic displacements in the charge ice pyrochlore $Bi_2Ti_2O_6O'$ studied by neutron total scattering. *Phys. Rev. B: Condens. Matter Mater. Phys.* **2010**, *81*, 144113.

(42) Shoemaker, D. P.; Seshadri, R.; Tachibana, M.; Hector, A. L. Incoherent Bi off-centering in $Bi_2Ti_2O_6O'$ and $Bi_2Ru_2O_6O'$: Insulator versus metal. *Phys. Rev. B: Condens. Matter Mater. Phys.* **2011**, *84*, 064117.

(43) Viehland, D.; Jang, S. J.; Cross, L. E. Freezing of the polarization fluctuations in lead magnesium niobate relaxors. *J. Appl. Phys.* **1990**, *68*, 2916−2921.

(44) Tagantsev, A. K. Vogel-Fulcher relationship for the dielectric permittivity of relaxor ferroelectrics. *Phys. Rev. Lett.* **1994**, *72*, 1100−1103.

(45) Nino, J. C.; Lanagan, M. T.; Randall, C. A. Dielectric relaxation in Bi_2O_3-ZnO-Nb_2O_5 cubic pyrochlore. *J. Appl. Phys.* **2001**, *89*, 4512−4516.

(46) Chu, F.; Reaney, I. M.; Setter, N. Investigation of relaxors that transform spontaneously into ferroelectrics. *Ferroelectrics* **1994**, *151*, 343−348.

(47) Shvartsman, V. V.; Lupascu, D. C. Lead-Free Relaxor Ferroelectrics. *J. Am. Ceram. Soc.* **2012**, *95*, 1−26.

(48) Lei, C.; Bokov, A. A.; Ye, Z.-G. Ferroelectric to relaxor crossover and dielectric phase diagram in the $BaTiO_3$-$BaSnO_3$ system. *J. Appl. Phys.* **2007**, *101*, 084105.

(49) Maiti, T.; Guo, R.; Bhalla, A. S. Structure-Property Phase Diagram of $BaZr_xTi_{1-x}O_3$ System. *J. Am. Ceram. Soc.* **2008**, *91*, 1769−1780.

(50) Ogihara, H.; Randall, C. A.; Trolier-McKinstry, S. Weakly Coupled Relaxor Behavior of $BaTiO_3$-$BiScO_3$ Ceramics. *J. Am. Ceram. Soc.* **2009**, *92*, 110−118.

(51) Bonneau, P.; Garnier, P.; Calvarin, G.; Husson, E.; Gavarri, J. R.; Heiwat, A. W.; Morell, A. X-ray and neutron diffraction studies of the diffuse phase transition in $PbMg_{1/3}Nb_{2/3}O_3$ ceramics. *J. Solid State Chem.* **1991**, *91*, 350−361.

(52) de Mathan, N.; Husson, E.; Gavarri, J. R.; Heiwat, A. W.; Morell, A. A structural model for the relaxor $PbMg_{1/3}Nb_{2/3}O_3$ at 5 K. *J. Phys.: Condens. Matter* **1991**, *3*, 8159−8171.

(53) Bing, Y.-H.; Bokov, A. A.; Ye, Z.-G. Diffuse and sharp ferroelectric phase transitions in relaxors. *Curr. Appl. Phys.* **2011**, *11*, S14−S21.

(54) Jonscher, A. K. *Universal Relaxation Law*; Chelsea Dielectrics Press: London, 1996.

(55) Ren, W.; Thayer, R.; Randall, C. A.; Shrout, T. R.; Trolier-McKinstry, S. Bismuth Pyrochlore Films for Dielectric Applications. *MRS Bull.* **1999**, *603*, 137−142.

(56) Hinojosa, B. B.; Nino, J. C.; Asthagiri, A. First-principles study of cubic Bi pyrochlores. *Phys. Rev. B: Condens. Matter Mater. Phys.* **2008**, *77*, 104123.

(57) Somphon, W.; Ting, V.; Liu, Y.; Withers, R. L.; Zhou, Q.; Kennedy, B. J. Local crystal chemistry, structured diffuse scattering and the dielectric properties of $(Bi_{1-x}Y_x)_2(M^{III}Nb^V)O_7$ (M = Fe^{3+}, In^{3+}) Bi-pyrochlores. *J. Solid State Chem.* **2006**, *179*, 2495−2505.

(58) Liu, Y.; Withers, R. L.; Welberry, T. R.; Wang, H.; Du, H. Crystal chemistry on a lattice: The case of BZN and BZN-related pyrochlores. *J. Solid State Chem.* **2006**, *179*, 2141−2149.

(59) Withers, R. L.; Welberry, T. R.; Larsson, A.-K.; Liu, Y.; Norén, L.; Rundlöf, H.; Brink, F. J. Local crystal chemistry, induced strain and short range order in the cubic pyrochlore $(Bi_{1.5-\alpha}Zn_{0.5-\beta})$-$(Zn_{0.5-\gamma}Nb_{1.5-\delta})O_{(7-1.5\alpha-\beta-\gamma-2.5\delta)}$ (BZN). *J. Solid State Chem.* **2004**, *177*, 231−244.

(60) Trump, B. A.; Koohpayeh, S. M.; Livi, K. J. T.; Wen, J.-J.; Arpino, K. E.; Ramasse, Q. M.; Brydson, R.; Feygenson, M.; Takeda, H.; Takigawa, M.; Kimura, K.; Nakatsuji, S.; Broholm, C. L.; McQueen, T. M. Universal geometric frustration in pyrochlores. *Nat. Commun.* **2018**, *9*, 2619.

(61) Subramanian, M. A.; Aravamudan, G.; Subba Rao, G. V. Oxide pyrochlores -a review. *Prog. Solid State Chem.* **1983**, *15*, 55−143.

(62) Ramirez, A. P. Strongly geometrically frustrated magnets. *Annu. Rev. Mater. Sci.* **1994**, *24*, 453−480.

(63) Rau, J. G.; Gingras, M. J. P. Frustrated Quantum Rare-Earth Pyrochlores. *Annu. Rev. Condens. Matter Phys.* **2019**, *10*, 357−386.